Modeling Time-Varying Variability and Reliability of Freeway Travel Time Using Functional Principal Component Analysis

Jeng-Min Chiou, *Member, IEEE*, Han-Tsung Liou, and Wan-Hui Chen

***Abstract*— This paper presents an aproach for modeling travel time variability and reliability that accounts for time-of-day effects on travel time variations. The conditional probability density functions of travel time in each specific period play a fundamental role in the modeling of time-varying variability and reliability. Nonparametric kernel density estimation is applied to travel time data, which enhances the flexibility and accuracy in accommodating travel time distributions under various complex traffic conditions. The proposed functional travel time density model (FTTDM) uses functional principal component analysis in kernel density function estimates for modeling and depicting time-varying variability through the dependence on the departure time of day. The resulting quantile estimates are used to obtain time-varying reliability, which considers the addition of extra time to the average or the median for an on-time arrival. This study uses linked travel time data of an electronic toll collection system to estimate route travel times in the Taiwan Freeway system. As illustrated in the data applications, the FTTDM effectively captures the time-varying feature of travel time variability and reliability, and the reliability indicators identify the unreliable departure time of day of a route.**

***Index Terms*— Electronic toll collection system, functional data analysis, kernel density estimation, quantile function, travel time variability, travel time reliability.**

I. Introduction

TRAVEL time information is essential in a transportation system. However, significant variations in travel time over a time-of-day period induced by variable travel demands and limited capacities create challenges for assessing travel time variability and reliability.

Travel time variability can be characterized by probability distributions, including standard deviation, skewness and kurtosis, coefficients of variation, and interquantiles of travel times [1]–[6]. It is a critical concern in transportation economics because it generates costs for road users [7]. Its value is influenced by time constraints; for example, it can be critical during morning peak travel hours [8].

Travel time variability can further serve as a basis for quantifying travel time reliability, which can be regarded as the extent of consistency over acceptable time for road users on a given route. Various definitions of travel time reliability have been proposed. These include the probability that travel times remain below an acceptable level [9], statistical range methods evaluating the spread of travel times around the expected value [10], and buffer time indices representing the distance between the travel time of the 90th percentile and the average [6]. These reliability indices measure the extent of unexpected delays and rely on realizations of probability distributions of travel times.

Large travel time variability implies low travel time reliability that becomes worse in the congestion state [6], [11]. Traffic instabilities such as speed oscillations and stop-and-go waves are common phenomena in congested traffic. Interactions between travel time variability and speed oscillation can be evaluated from microscopic features of traffic flow [2], [12]. Travel time variability negatively correlates with traffic speed yet positively correlates with traffic density. It increases with flow rate when it is below the maximum flow rate but is inversely correlated when it reaches the capacity [13].

Probability distributions of travel time vary with the time of day, and thus, it is plausible to model travel time density functions as a function of departure times to capture their time trends and variations within a day. To model the temporal variations of travel times with the complex time-varying feature, we propose using functional data analysis (FDA) to model the conditional densities of travel times as functions of time of day coupled with nonparametric kernel density estimates. We assume that the estimated probability density functions of travel time, conditional on specific departure times, are random trajectories that reflect stochastic variations and time-varying changes in travel time. This random function point of view forms the basis for the FDA approach, which takes the conditional density functions as the basic unit for statistical analysis. To the best of our knowledge, no studies have modelled the time-varying feature of dynamic travel time variability and reliability using an FDA approach.

FDA has been extensively developed as a statistical methodology to analyze data that are in the form of functions, curves, or more general objects. Systematic overviews of FDA

Manuscript received February 8, 2019; revised September 3, 2019 and October 7, 2019; accepted November 18, 2019. Date of publication December 5, 2019; date of current version December 24, 2020. This work was supported in part by the Academia Sinica under Grant AS-IA-105-M01 and in part by the Ministry of Science and Technology, Taiwan, under Grant MOST 107-2118-M-001-001-MY3. The Associate Editor for this article was B. Seibold. *(Corresponding author: Jeng-Min Chiou.)*

J.-M. Chiou and H.-T. Liou are with the Institute of Statistical Science, Academia Sinica, Taipei City 11529, Taiwan (e-mail: jmchiou@stat.sinica.edu.tw).

W.-H. Chen is with the Department of Transportation Management, Tamkang University, New Taipei City 25137, Taiwan.

Digital Object Identifier 10.1109/TITS.2019.2956090

have been provided in monographs [14], [15] and review articles [16], [17]. Among the various topics in this field, functional regression analysis is widely applied when either one or both of the predictor and response variables contain random functions. For example, dynamical functional prediction for traffic flow was developed using functional regression analysis when both the predictor and response are random functions [18]. Here, we consider the case of a functional response variable, the travel time density function, with a scalar predictor, departure time of day. The literature of this type of regression includes applications to the covariate effects on medfly egg-laying profiles [19] and the effect of birth year on cohort mortality forecasts [20], among others.

This study uses linked travel time data from an electronic toll collection (ETC) system to estimate route travel times. The ETC travel time data are collected based on the empirical observations obtained by the technology of automatic vehicle identifications. The corresponding traffic speed of ETC is the space-mean speed rather than the time-mean speed as recorded by vehicle detectors or video cameras. Travel time estimation inferred from time-mean speed data requires considerations on various traffic states to reduce systematic biases [21], [22], whereas the biases due to time-mean speed were theoretically investigated and empirically verified by the ETC actual speed records [23]. In contrast, the ETC travel time data are more accurate irrespective of the traffic state.

We use travel time data from the Taiwan Freeway Traffic Data Collection System (TDCS) to model travel time densities as departure time-of-day functions for investigating time-varying changes in the variability and reliability. We develop a data-adaptive statistical modeling approach and a data-analytic tool with which to study travel time variability and reliability.

A. Data and ETC-linked Route Travel Time Estimation

The TDCS collects travel time information by matching vehicle license plates between two consecutive ETC gates and averaging the travel times of passing vehicles to obtain aggregated travel time records based on a 5-min time window. The Taiwan ETC system has been migrated to the fully automatic system since 2014, with distance-based pricing supported by electronic tolling. Thus, the traffic volume used to calculate the 5-min aggregated travel times are population-based. Moreover, the ETC has more than 6 million registered vehicles since then with the toll collection rates above 99.9% [24], yielding a sufficiently large sample to collect travel time data. The TDCS provides an online archived traffic database called TISVCLOUD (http://tisvcloud.freeway.gov.tw/) that stores current and historical traffic data. The M04A dataset in TISVCLOUD comprises average ETC travel times based on vehicle type between consecutive ETC gates. To obtain the travel time for a route with a specific origin and destination that extends beyond two consecutive ETC gates, we need to link the travel time records while considering time shifts due to vehicle movement. We propose an algorithm for calculating route travel time between a prespecified origin and destination ETC gates for a given start time window. The key idea is to correctly link the ETC records to a subsequent time window for each ETC segment in order to obtain a linked travel time.

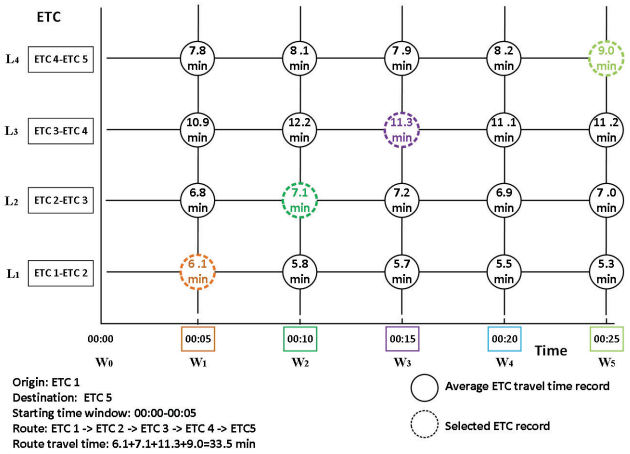

Fig. 1. Pseudo travel time records of two consecutive ETC gates for different time windows.

Fig. 1 illustrates the calculation of the travel time from ETC_1 to ETC_5. The values in circles represent the average travel time for the time window between two consecutive ETC gates. A travel time of 6.1 min is required from ETC_1 to ETC_2 at [0:00, 0:05), which links to the next time window of [0:05, 0:10), yielding a travel time of 7.1 min from ETC_2 to ETC_3. Thus, the travel time from ETC_1 to ETC_3 is 13.2 min, which subsequently links to the time window of [0:10, 0:15), yielding a travel time of 11.3 min from ETC_3 to ETC_4. Therefore, the travel time from ETC_1 to ETC_4 is 24.5 min, which in turn links to the time window of [0:20, 0:25), yielding a travel time of 9 min from ETC_4 to ETC_5. Consequently, a traveler departing at [0:00, 0:05) and traveling from the origin, ETC_1, to the destination, ETC_5, requires 33.5 min. The algorithm for calibrating linked travel time in shown Algorithm 1.

Algorithm 1 ETC Linked Route Travel Time

Parameters and input data:
ETC_i: the ith ETC gate from the origin, ETC_o, to the destination, ETC_d;
L_i: the ith ETC segment between ETC_i and $\text{ETC}_{(i+1)}$;
W_j: the jth 5-min time interval, where $j = 1, \ldots, M$;
$\text{ETT}(L_i, W_j)$: the ETC travel time of L_i at W_j;
$\text{ERT}(W_s)_\ell^k$: the estimated route travel time departing at time W_s and traveling from locations ETC_ℓ to ETC_k;
begin
  Set the departure time W_s;
  Initialize $\text{ERT}(W_s)_o^d = 0$;
  Set $j = s$;
  for $i = o$ **to** $(o + d - 1)$ **do**
    $j = j + \lfloor \text{ERT}(W_{(j+1)})_{(i-1)}^i / 5 \rfloor$;
    $\text{ERT}(W_s)_o^d = \text{ERT}(W_s)_o^d + \text{ETT}(L_i, W_j)$;
  end for
end

Using the TDCS data in 2014, we study two sections in the Taiwan freeway system. The Taipei-to-Taichung (southbound)

route on Freeway No. 1. is approximately 151 km, including 33 ETC gates. The Yilan-to-Taipei (northbound) route across Freeways No. 5 (31 km), 3 (5 km), and 3A (4 km) is about 40 km, passing through seven ETC gates and five tunnels, including the longest Hsueh-Shan tunnel 12.9 km. Taipei and Taichung are the major metropolises in northern and central Taiwan, respectively, whereas Yilan County is located in northeastern Taiwan, with tourist attractions.

Besides, we also apply the modeling methodology to the travel time data of Sonoma US-101-N with a path from Vista Point (Marin County) to Redwood (Sonoma County) for approximately 130 km. The data are available from the Caltrans Performance Measurement System (PeMS) [25] that provides the travel time data calculated based on the speed measurements collected by vehicle loop detectors. Although ETC travel time data are our focus, we use this data set to show the broad applicability of the methodology.

The remainder of this paper is structured as follows. Section II presents the modeling approach for travel time variability and reliability using functional principal component analysis for the conditional density functions. Section III provides the methods of estimating the components of the proposed model. Section IV demonstrates the numerical results of the real data applications. Finally, Section V summarizes the research with concluding remarks and discussions.

II. Proposed Methods

We model travel time distributions through conditional probability density functions that form the basis for using FDA to capture time-varying changes of travel time variability and reliability. Because a route's travel time depends on the time of day, we take it as a function of the departure time. We consider the conditional travel time density functions at each time-of-day period to be random functions because travel times are themselves stochastic. The conditional travel time density functions in a time-of-day period can be represented by the Karhunen–Loève representation [17], [26]. We incorporate the departure time-of-day influence on these random density functions through the conditional expectation of the stochastic representation. The probability density functions of travel times are estimated using distribution-free kernel density function estimation [27], and the quantiles of the distributions are further derived from the probability density functions.

A. Stochastic Representation of a Random Function

Let $f(x)$ be a random function with support on a common interval $\mathcal{X}$. In this study, $f(x)$ corresponds to a derived density function of travel time x; its realization cannot be observed directly, and thus, it must be estimated. For FDA, we assume that the random function $f(x)$ is continuous and square integrable in $L_2(\mathcal{X})$; that is, $\int_{\mathcal{X}} E\left\{f^2(x)\right\} dx < \infty$. For any functions f and g in $L_2(\mathcal{X})$, define the inner product $\langle f, g\rangle = \int_{\mathcal{X}} f(x)g(x)dx$.

The Karhunen–Loève representation decomposes the random function into fixed and random parts:

$$f(x) = \mu(x) + \sum_{j=1}^{\infty} \xi_j \phi_j(x). \tag{1}$$

The fixed part is the mean function $\mu(x) = E\{f(x)\}$ that is smooth (twice continuously differentiable); the random part comprises the sum of the random components, which is a linear combination of a set of basis functions coupled with random coefficients. The basis functions $\{\phi_j, j = 1, 2, \ldots\}$ in $L_2(\mathcal{X})$ are orthonormal and smooth, satisfying $\langle \phi_j, \phi_l\rangle = \delta_{jl}$, where δ_{jl} is the Kronecker symbol with 1s if $j = l$ and 0s otherwise. The random coefficients or principal components $\xi_j = \langle f - \mu, \phi_j\rangle$ are uncorrelated with mean $E(\xi_j) = 0$ and variance $\text{var}(\xi_j) = \lambda_j$. The first principal component ξ_1 represents the length of the projection of $(f - \mu)$ onto ϕ_1, and $\xi_1\phi_1$ explains the maximum amount of the process variance in f among all functions involving a single real-valued random variable. Analogously, $\xi_2\phi_2$ explains the additional maximum amount of variance unexplained by $\xi_1\phi_1$, and so on.

The basis functions $\{\phi_j\}$ are associated with the covariance operator $G(\cdot, \cdot)$ of $f(\cdot)$ and satisfy the eigendecomposition $\langle G(x, \cdot), \phi_j\rangle = \lambda_j\phi_j(x)$. Here, for notational convenience, we do not distinguish the covariance function $G(\cdot, \cdot)$ from the covariance operator. The autocovariance function of f at any two points x and x' in $\mathcal{X}$, $\text{cov}\left\{f(x), f(x')\right\}$, has the spectral decomposition

$$G(x_1, x_2) = \sum_{j=1}^{\infty} \lambda_j \phi_j(x_1)\phi_j(x_2). \tag{2}$$

The eigenvalues λ_j are nonincreasing in j with the property that $\sum_{j=1}^{\infty} \lambda_j < \infty$ for an L_2 process. The realizations of the random coefficients ξ_j are the functional principal component (FPC) scores.

The convergence of the sum in (1) holds uniformly such that $\sup_{x\in\mathcal{X}} E\{f(x) - \mu(x) - \sum_{j=1}^{K} \xi_j\phi_j(x)\}^2$ converges to zero as $K \to \infty$. In practice, only a finite number of realizations in each data object are recorded even though the random function is infinite dimensional, and the FPCs corresponding to small values of $\{\lambda_j\}$ close to zero may not contribute significantly to the sum of the infinite series. It then leads to a truncated version of (1),

$$f^K(x) = \mu(x) + \sum_{j=1}^{K} \xi_j \phi_j(x). \tag{3}$$

Here, the integer K must be chosen appropriately to ensure that the first K terms yield an accurate approximation of the infinite sum. The expansion (1) facilitates dimension reduction from the infinite sum to the first K terms for a large enough K; thus, the information contained in $f(\cdot)$ is essentially composed of the K-dimensional vector $(\xi_1, \ldots, \xi_K)$ in (3). Therefore, the vector of the principal components serves as a proxy for the infinite-dimensional function of $f(\cdot)$ in (1).

B. Functional Travel Time Density Model

The proposed functional travel time density model (FTTDM) formulates the influence of departure time of day T through the FPCs, with the conditional expectation

$$E\{f(x) \mid T\} = \mu(x) + \sum_{j=1}^{\infty} E(\xi_j \mid T)\phi_j(x), \tag{4}$$

where $\mu(x)$ is the overall mean function as in (1), and $\phi_j(x)$ is the basis function satisfying the spectral decomposition of the conditional covariance function,

$$G(x, x' \mid T = t) = \operatorname{cov}\left\{f_t(x),\, f_t(x')\right\} = \sum_{k=1,l=1}^{\infty} E(\xi_k \xi_l \mid T = t)\phi_k(x)\phi_l(x'). \quad (5)$$

Because the eigenfunctions $\{\phi_j\}$ are independent of the covariate T, the conditional covariance (5) implies that the basis functions $\{\phi_j\}$ also satisfy the spectral decomposition of the marginal autocovariance function in (2).

Let $E(\xi_j \mid T = t) = \eta_j(t)$ be the conditional expectation of the random coefficient ξ_j at $T = t$ and assume that $\eta_j(t)$ is a smooth function in time-of-day t. The function $\eta_j(t)$ reflects the time-of-day changes in the travel time density functions. The FTTDM in (4) is an extension of the classical Karhunen–Loève expansion in (1). It incorporates the influence of the time-of-day covariate effect T through the conditional distribution of the principal components $\{\xi_j\}$, the random effects in the model, via the smooth regression relationship between ξ_j and T.

C. Travel Time Reliability and Conditional Quantile Functions

Let $f_t(x) = f(x \mid T = t)$ denote the probability density function conditional at the time-of-day period $T = t$, satisfying $\int_{-\infty}^{\infty} f_t(x)\mathrm{d}x = 1$. The conditional travel time distribution function $F_t(\cdot)$ at the covariate $T = t$ is obtained using $f_t(\cdot)$ as follows:

$$F_t(x) = F(x \mid T = t) = \int_{-\infty}^{x} f_t(z)\ \mathrm{d}z. \quad (6)$$

The $100u\%$ quantile of the conditional travel time distribution is given by

$$Q_t(u) = Q(u \mid T = t) = F_t^{-1}(u) = \inf\{x : F_t(x) \geq u\}, \quad (7)$$

where $0 \leq u \leq 1$.

Whereas the conditional travel time distribution functions in (6) are useful for quantifying travel time variability, the conditional quantile functions in (7) also serve as a useful measure for reflecting travel time variability; furthermore, they can be used to quantify travel time reliability. Among various indices defined for travel time reliability, the notion of buffer time is commonly incorporated by road users when planning trips in consideration of travel time variability. The buffer time measures the deviation in travel time from the average value [6], [28]. However, when the travel time distribution is skewed, it is appropriate to replace the referenced average value with its median. We extend the conventional buffer time index (BTI) to a robust time-varying travel time reliability function using the FTTDM and the quantiles.

The BTI indicates the extra percentage of time required compared with the average or median travel time, which is straightforward and easy to understand. The BTI, conditional on the departure time-of-day $T = t$, is defined as

$$\mathrm{BTI}_t(u; M_t) = \frac{Q_t(u) - M_t}{M_t}, \quad (8)$$

where $Q_t(u)$ is the $100u\%$ conditional quantile of travel time at $T = t$, with u restricted to $u > 0.5$. The reference quantity M_t can be the mean $M_t = \int_{-\infty}^{\infty} z f_t(z)\mathrm{d}z$ or the median $M_t = Q_t(0.5)$. The buffer time uses the average or median travel time as a reference for calculating the percentage difference between the $100u$ percentile of the travel time and the reference travel time. It represents the extra time that most travelers should add on ($100u$ percent) to the reference travel time to arrive on time. When the conditional travel time distribution is skewed or the realizations of travel time contain many outliers, as is often the case, BTI relative to the median travel time is recommended. The BTI value increases as the reliability decreases; specifically, a low BTI value indicates a highly reliable travel time.

Besides, we also consider the two robust measures of travel time reliability, the *width* and the *skewness* [6], which are based he quantiles of the distributions as well,

$$\lambda_t^{var} = \frac{Q_t(0.9) - Q_t(0.1)}{Q_t(0.5)}, \quad \lambda_t^{skew} = \frac{Q_t(0.9) - Q_t(0.5)}{Q_t(0.5) - Q_t(0.1)}. \quad (9)$$

The width index λ_t^{var} depicts the ratio of the range of the central 80% observations to the median travel time, which is similar to the robust $\mathrm{BTI}_t(0.9; M_t)$ yet concerning the higher quantile range above the median instead. The skewness index λ_t^{skew} presents the relative chance of extreme travel times between the 90th and the 10th percentiles relative to the median of the distribution.

III. Estimation of Model Components

The conditional density function of travel time $f_t(x)$ is unknown and must be estimated. We use the observations of travel time to estimate the conditional densities and quantiles of travel time for each time-of-day period. Let $T = t_1, \ldots, t_M$ be the observed time points and $\{X_{t_k,i}; i = 1, \ldots, n\}$ denote the observations of travel time at the time-of-day period t_k, $k = 1, \ldots, M$, for day i. Our application features $M = 216$ time points with 5-min intervals from 06:00 to 23:59.

A. Nonparametric Kernel Density Estimation

In the literature, typical parametric forms of probability distribution functions used to fit travel time data include normal, lognormal, gamma, Weibull, and Gaussian mixture (GMM) models [2], [5], [10], [29]–[31].Nevertheless, assuming a particular parametric travel time distribution model may be inadequate because a single model cannot satisfactorily accommodate various traffic conditions for different road segments and periods, and inaccurate probability distribution models may limit applications to travel time analyses [6], [29]. The nonparametric kernel density estimation for travel time distributions, which is data adaptive, can relax this constraint [32]–[34]. In our numerical results to be shown later, these parametric models indicate a significant lack of model fit, whereas the kernel density estimates pass goodness-of-fit tests.

Using kernel density estimators, we obtain a smooth density function estimate of $f_T(x)$ at each $T = t_1, \ldots, t_M$, evaluated

at the range of travel times x by

$$\tilde{f}_{t_k}(x) = \frac{1}{nh}\sum_{i=1}^{n} K\left(\frac{x - X_{t_k,i}}{h}\right), \tag{10}$$

where $K(\cdot)$ is the kernel function and h is the bandwidth ($h \to 0$ as $n \to \infty$), which can be selected using a leave-one-point-out cross-validation method. The real-valued kernel function $K(\cdot)$ is nonnegative definite and symmetric around zero; has finite support such that $K(x) = 0$ for $|x| > c$, where $c > 0$ is a constant; and satisfies $\int_{-\infty}^{\infty} K(x)\mathrm{d}x = 1$ and the Lipschitz condition. Commonly used kernel functions include Epanechnikov, triangular, biweight, and uniform kernels [27].

Because the support of $f_T(x)$ at each $T = t_k$ can differ, we determine the range of support by taking the minimum x_1 and maximum x_L across all supports of the conditional density estimates $\tilde{f}_{t_k}(x)$, for $k = 1, \ldots, M$. Let the common support be the closed interval $\mathcal{X} = [x_1, x_L]$. We evaluate the conditional densities at 100 equally spaced points $\{x_i\}$ in $\mathcal{X}$ with $L = 100$. Thus, the kernel density estimates $\{\tilde{f}_{t_1}(x), \ldots, \tilde{f}_{t_M}(x)\}$ in (10), evaluated at $x \in \mathcal{X}$ and conditional on each time-of-day period $T = t_1, \ldots, t_M$, are used as realizations of the random functions $f_T(x)$ conditional on $T = t_k$ for further modeling and analysis.

B. Estimation of Model Components

We perform FPC analysis on the set of estimated density functions. We obtain the estimates of the mean function $\hat{\mu}(x)$ and covariance function $\hat{G}(x, x')$ through one- and two-dimensional local polynomial regression [35]. For the mean function, we use local linear smoothing by minimizing

$$\sum_{k=1}^{M}\sum_{l=1}^{L} K_\mu\left(\frac{x - x_l}{h_\mu}\right)\left\{\tilde{f}_{t_k}(x_l) - \alpha_0 - \alpha_1(x - x_l)\right\}^2, \tag{11}$$

for all x, with respect to (α_0, α_1), where K_μ is the kernel function and h_μ is the bandwidth. The resulting mean function estimate $\hat{\mu}(x) = \hat{\alpha}_0(x)$ is the minimizer of (11). Let $G_k(x_l, x_{l'}) = \{\tilde{f}_{t_k}(x_l) - \hat{\mu}(x_l)\}\{\tilde{f}_{t_k}(x_l') - \hat{\mu}(x_l')\}$ for $1 \le l, l' \le L$. For the covariance function, we minimize

$$\sum_{k=1}^{M}\sum_{1\le l\ne l'\le L} K_c\left(\frac{x - x_l}{h_c}, \frac{x' - x_{l'}}{h_c}\right)\{G_k(x_l, x_{l'}) - \beta_0 - \beta_{11}(x - x_l) - \beta_{12}(x' - x_{l'})\}^2, \tag{12}$$

for all (x, x'), with respect to $(\beta_0, \beta_{11}, \beta_{12})$, where K_c is the bivariate kernel function and h_c is the bandwidth. The resulting covariance function estimate $\hat{G}(x, x') = \hat{\beta}_0(x, x')$ is the minimizer of (12). Here, we use the leave-one-curve-out cross-validation method to obtain the bandwidths h_μ and h_c.

The estimated eigenvalues $\hat{\lambda}_j$ and the orthonormal eigenfunctions $\{\hat{\phi}_j(x)\}$ are obtained through discrete approximations to the solutions of the eigen-equations $\langle \hat{G}(\cdot, x), \hat{\phi}_j\rangle = \hat{\lambda}_j\hat{\phi}_j(x)$. The FPC scores $\{\hat{\xi}_{t_k,j}; k = 1, \ldots, M\}$ can be obtained using numerical approximations to the inner product $\langle \tilde{f}_{t_k} - \hat{\mu}, \hat{\phi}_j\rangle$. The estimated conditional mean function $\hat{\eta}_j(t)$ of $E\{\xi_j \mid T = t\}$ is obtained using a local linear smoother that minimizes

$$\sum_{k=1}^{M} K_\xi\left(\frac{t_k - t}{h_\xi}\right)[\hat{\xi}_{t_k,j} - \{\gamma_0 + \gamma_1(t_k - t)\}]^2 \tag{13}$$

for all t, with respect to (γ_0, γ_1). This yields $\hat{\eta}_j(t) = \hat{\gamma}_0(t)$, the minimizer of (13) at t. Here, K_ξ is the kernel function, and h_ξ is the bandwidth used for the local linear smoother. FPC analysis techniques have been widely used in FDA. See [17], [18] for examples of more detailed descriptions of estimation and related applications.

Subsequently, the fitted conditional travel time density estimates of FTTDM (4) are obtained using

$$\hat{f}_t(x) = \hat{\mu}(x) + \sum_{j=1}^{L}\hat{\eta}_j(t)\hat{\phi}_j(x), \tag{14}$$

where L is chosen according to a selection criterion. L is commonly chosen on the basis of the proportion of variance explained by the FPCs;

$$L = \arg\min\left\{K : \sum_{j=1}^{K}\hat{\lambda}_j \Big/ \sum_{j=1}^{\infty}\hat{\lambda}_j \ge \delta\right\}, \tag{15}$$

where δ is chosen as 0.95 in this study, indicating that the first L components explain $100\delta\%$ of the total variance.

The conditional distribution function is estimated using discrete approximations to

$$\hat{F}_t(x) = \int_{-\infty}^{x}\hat{f}_t(u)\ \mathrm{d}u,$$

and the conditional quantile estimator of travel time is obtained by

$$\hat{Q}_t(u) = \hat{F}_t^{-1}(u) = \inf\{x : \hat{F}_t(x) \ge u\}, \quad 0 \le u \le 1. \tag{16}$$

The estimator of the time-varying BTI, conditional on time $T = t$, is obtained by

$$\widehat{\mathrm{BTI}}_t(u; M_t) = \frac{\hat{Q}_t(u) - \hat{M}_t}{\hat{M}_t}, \tag{17}$$

where $\hat{Q}_t(u)$ is the estimated $100u\%$ quantile, and $\hat{M}_t = \int_{\mathcal{X}} x\hat{f}_t(x)dx$ is the estimated mean or $\hat{M}_t = \hat{Q}_t(0.5)$ the estimated median.

IV. Real Data Application to Estimating Travel Time Variability and Reliability for a Freeway

We illustrate the results for the Taipei-to-Taichung route in more detail, whereas showing only the selected quantiles and the reliability indicators for the Yilan-to-Taipei and the Sonoma-US-101 routes due to limited space. Because traffic characteristics on Saturdays and Sundays differ from those on work days, we divide the daily travel time records into four exclusive groups: regular weekdays (Mondays–Thursdays), Fridays, Saturdays, and Sundays. We exclude weekdays that are public holidays because their traffic patterns generally differ from those of the four types of day.

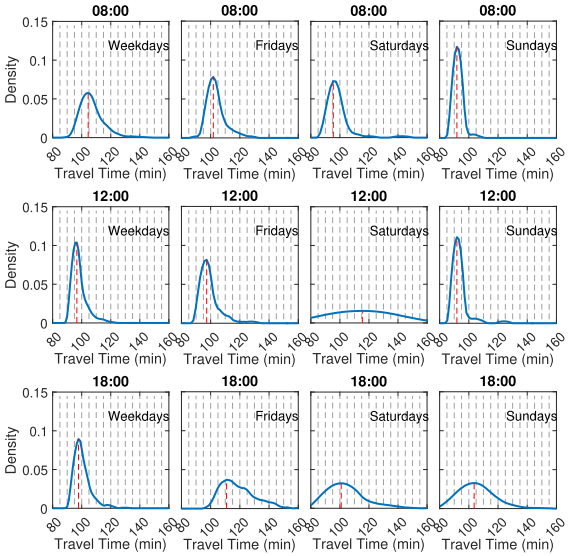

Fig. 2. Kernel density function estimates using (10) of the travel times departed at 08:00, 12:00 and 18:00 (row-wise; top to bottom) for regular weekdays, Fridays, Saturdays, and Sundays (column-wise; left to right) of the Taipei-to-Taichung route.

A. Kernel Density Function Estimates of Travel Time

Fig. 2 illustrates the estimated kernel density functions, using (10), for travel times of the Taipei-to-Taichung route at 08:00, 12:00, and 18:00 for the four types of day. The peak of a density curve corresponds to the mode of travel time, and a density curve with a wide spread indicates considerable variability.

Fig. 2 shows evident differences in shape not only among the types of day but also among departure times. For each of the four types of day, the modes and shapes of the conditional density functions vary significantly with time-of-day periods. The density functions at 08:00 reveal slightly smaller modes of travel time with shorter spreads on weekends than on weekdays. The density functions at 12:00 on weekends indicate unstable travel times compared with those on weekdays. The evening traffic (18:00) exhibits distinct density function shapes, indicating different extents of traffic jams, particularly on weekends and Fridays. Therefore, it is plausible to model travel times through kernel density functions with flexible shapes depending on the departure time to reflect the time-varying feature of travel time.

B. Comparisons With Parametric Models of Travel Time

We compare the kernel density estimates of travel time with the parametric density models, including normal, lognormal, Weibull, gamma densities and Gaussian mixture model (GMM). Fig. 3 demonstrates discrepancy between each fitted parametric model and the kernel density estimates. Table I presents the Kolmogorov-Smirnov tests [36] for the goodness of fit (GOF) of each model based on the 216 probability density functions conditional on the departure time of day. The outcome indicates a severe lack of fit for the parametric density models, whereas almost all the kernel density estimates pass the GOF tests. Although the GMM generally fits better than

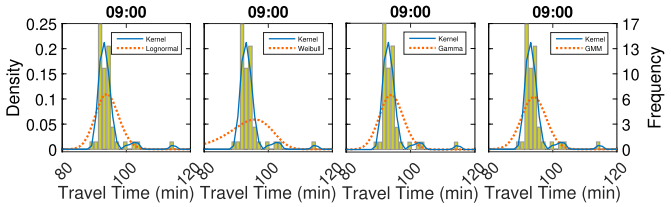

Fig. 3. Comparisons between the fitted parametric density functions (lognormal, Weibull, gamma, and GMM) and the kernel density estimates superimposed on the histograms of the travel times on weekdays departed at 09:00 for the Taipei-to-Taichung route.

TABLE I

NUMBERS OF PASSING THE KOLMOGOROV-SMIRNOV TESTS (OUT OF 216) ON THE PROBABILITY MODELS (LN: LOGNORMAL; WB: WEIBULL; GA: GAMMA; NO: NORMAL; GMM: GAUSSIAN MIXTURE MODEL) FOR THE TRAVEL TIME DATA FOR (A) TAIPEI-TO-TAICHING AND (B) YILAN-TO-TAIPEI ROUTES

Route	Day type	LN	Wb	Ga	No	GMM	Kernel
(A)	Weekdays	9	4	9	9	25	211
	Fridays	77	21	72	69	110	216
	Saturdays	86	34	81	72	97	216
	Sunday	89	28	89	85	111	216
(B)	Weekdays	8	0	7	4	27	216
	Fridays	112	40	100	89	122	216
	Saturdays	146	88	141	138	165	215
	Sunday	147	146	153	160	172	212

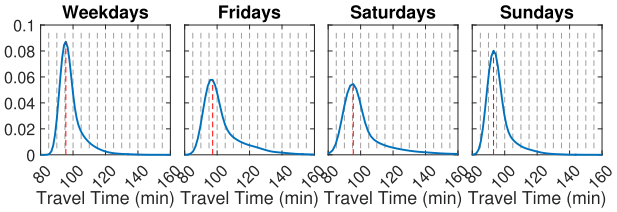

Fig. 4. Estimated mean functions of travel time densities for the Taipei-to-Taichung route.

other parametric models, it is still not comparable to the kernel density estimates. The comparison justifies the kernel density estimates are adequate for modeling travel time distributions.

C. Functional Principal Component Analysis for Probability Density Functions of Travel Times

This section illustrates the estimated components of the FTTDM (4) for the Taipei-to-Taichung route. Fig. 4 displays the estimated mean functions using the one-dimensional local polynomial smoothing method in (11). These are the marginal mean functions without considering the time-of-day effect on travel time. The spreads shown in the density functions indicate that travel times on Fridays and Saturdays are more variable than those on weekdays and Fridays, and the modes of the density functions center around 95 min.

Fig. 5 displays the estimated covariance functions. These covariance functions reflect the fluctuation and auto-correlation of the density functions. They are used to obtain the eigenfunctions $\{\hat{\phi}_j(t); j = 1, \ldots, L\}$ via spectral decompositions and the associated FPC scores

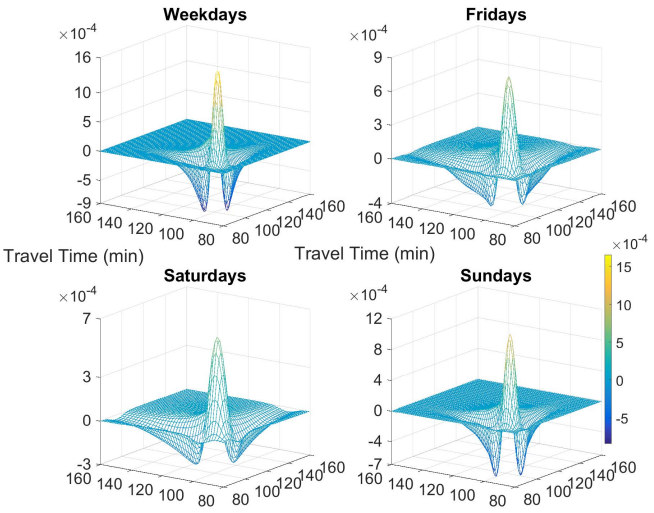

Fig. 5. Estimated covariance functions of travel time densities for the Taipei-to-Taichung route.

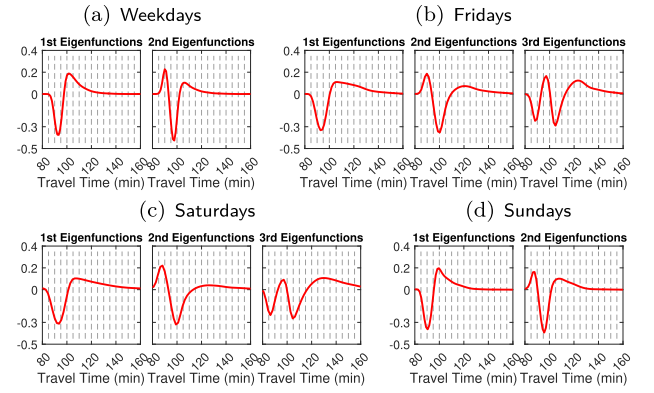

Fig. 6. Estimated eigenfunctions $\hat{\phi}_j(t)$ for travel times of the Taipei-to-Taichung route, with the total number of components selected by the 95% proportion-of-variance-explained criterion using (15).

$\{\hat{\xi}_{t_k,j}; k = 1,\ldots,M, j = 1,\ldots,L\}$, as illustrated in Figs. 6 and 7. Using the proportion-of-variance-explained criterion in (15) with a threshold value of 95%, three FPCs are selected for Fridays and Saturdays and two for weekdays and Sundays. The peaks and troughs of the eigenfunctions reflect the directions of variation for each FPC component at various values of travel time, and the corresponding FPC scores reflect the sizes of each individual variation in the density functions.

Most importantly, the FPC scores displayed as a function of departure times, along with the conditional expectations of the random coefficients $\{\hat{\eta}_j(t); j = 1,\ldots,L\}$ obtained using (13), clearly demonstrate the time-varying feature of the FPCs, as shown in Fig. 7. The FPCs vary with departure time of day, which reflects the time-dependent characteristic of travel time variability. In Fig. 7(a), for example, the first component of the conditional FPC scores shows the main peak hours at approximately 8:30 and 18:30, and the second component reveals the secondary peaks in the afternoon at approximately 15:00. The differences in travel time patterns among the four types of day support the strategy of subgroup analysis.

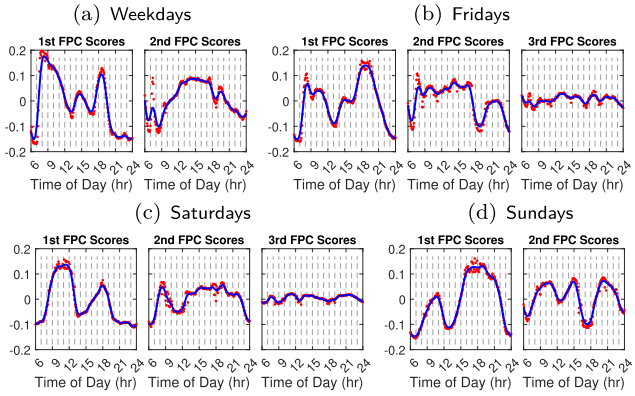

Fig. 7. Estimated conditional expectation $\hat{\eta}_j(t)$ using (13) superimposed on the FPC scores, associated with the eigenfunctions in Fig. 6.

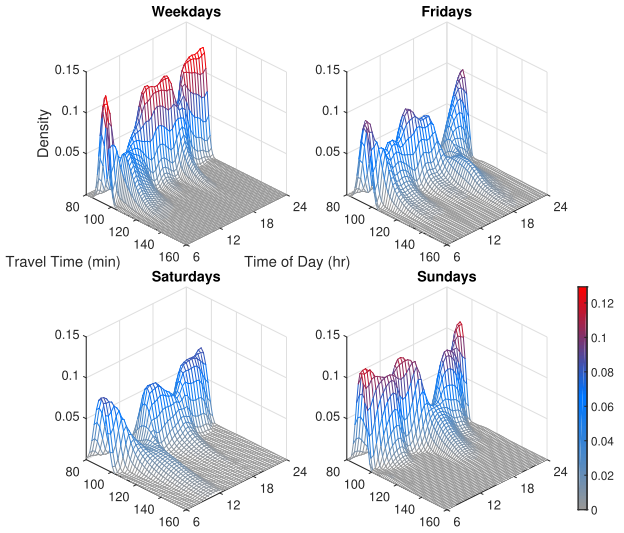

Fig. 8. Fitted travel time density surfaces of the Taipei-to-Taichung route.

D. Fitted Functional Travel Time Density Models

Figs. 8 displays the 3-dimensional surfaces of the fitted FTTDM, using (14), for the Taipei-to-Taichung route as a function of departure time of day. These surfaces characterize the temporal dynamics of travel time density functions with the time-varying feature on departure time. The cross-sectional curve at a specific time-of-day period corresponds to the conditional density function. Density functions with wider spreads indicate larger travel time variations; those with right-shifted modes show longer travel times, and vice versa.

The travel time density surfaces demonstrate dynamic changes in travel time distributions with departure time of day. The density curves exhibit two heavy tails on weekdays, indicating traffic congestion during peak hours (at approximately 09:00 and 18:00). On Fridays, the evening peak-hour traffic at approximately 18:00 is more severe than the morning peak-hour traffic. On Saturdays, the spread of the density function increases considerably with the period in the morning, indicating significant variations and longer travel times for departures at later morning hours; this is not observed on Sundays. The dynamic changes in the travel time density

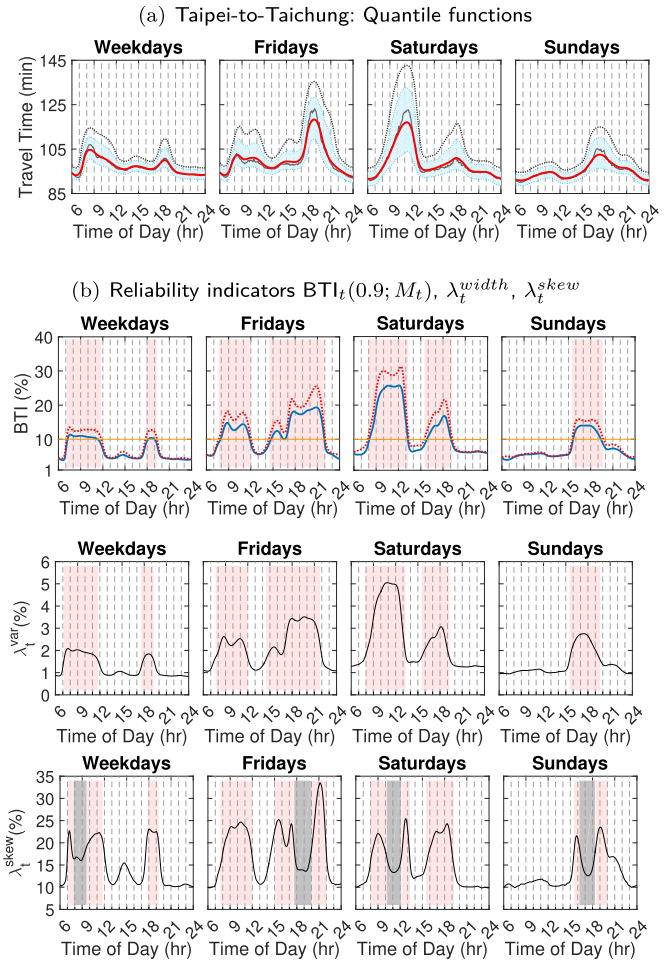

Fig. 9. (a) The estimated 85% quantile (dashed black) and the median function (solid red), superimposed on the sample medians (dotted curves) and enveloped by the 25th and the 75th percentile functions (shaded areas); (b) the reliability indicators BTI$_t(0.9; M_t)$ with M_t as mean (dotted red) and median (solid) (row 2), the width λ_t^{var} (row 3), and the skewness λ_t^{skew} (bottom row) for the Taipei-to-Taichung route.

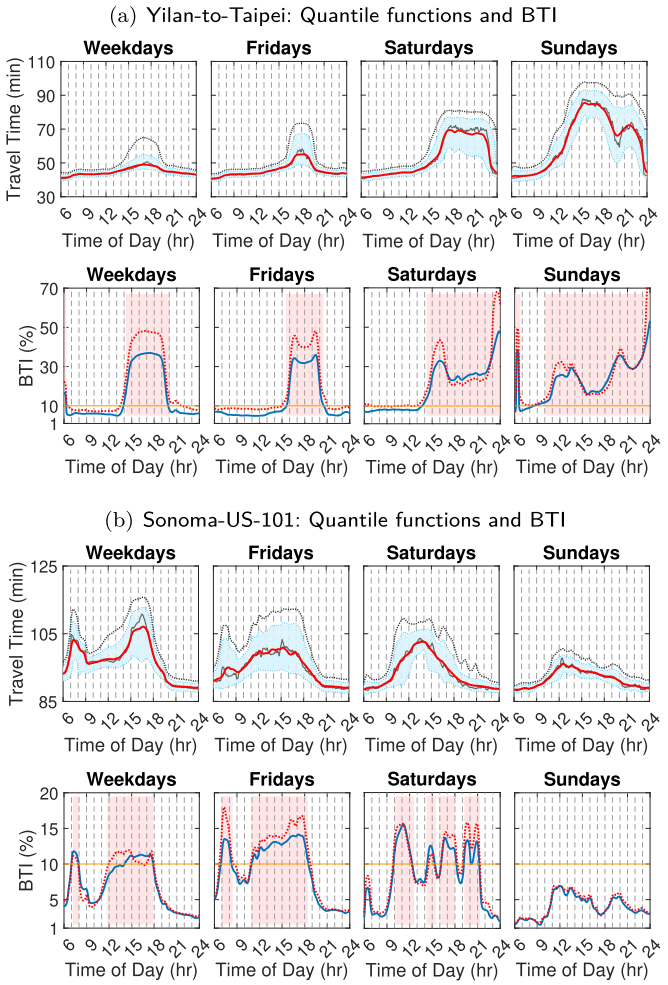

Fig. 10. The estimated quantile functions and the reliability indicators for (a) the Yilan-to-Taipei route and (b) the Sonoma-US-101 route, with a similar layout to Fig. 9.

functions with time of day reveal the time-varying feature of travel time variability, which also suggests that travel time reliability has time-varying characteristics. On Sundays, considerable variations occur from 17:00 to 18:00.

E. Quantile Functions and Travel Time Reliability

The quantile functions of travel time distributions obtained using (16) as a function of departure time of day are useful for depicting the dynamics of travel time variability. The estimated median (50% quantile) functions for travel times are shown in Fig. 9(a). The median curves of travel time indicate different peak hours among the four types of day, covered by the shaded bands of the 25th and 75th percentiles: the widths of the bands suggest their variability. The sample median curves (dashed) are superimposed on the fitted median functions, indicating that they are close to each other with slightly more significant discrepancies during peak hours. These figures clearly indicate that the route is frequently used during weekday mornings and Friday evenings, thereby causing longer travel times than other time periods. The traffic patterns generally show morning and evening peak-hours. In particular, during the peak periods with large variations (e.g., 15:00 to 21:59 on Sundays northbound), the 75% and 85% quantile travel times are much higher than the median travel times. Unreliable travel times generate costs for road users; therefore, we suggest providing travel time information with the median travel times along with higher quantiles (e.g., the 85% quantile or higher) of travel time. The time-varying quantile functions facilitate the use of travel time reliability indices to identify traffic congestion periods.

Fig. 9(b) demonstrates the 0.90 quantile time-varying BTI as well as the width and the skewness indicators for travel time reliability. The BTI values with reference to the mean and median functions suggest parallel patterns with considerable discrepancy at periods with longer travel times. We suggest the robust BTI using the median as the reference function because travel time distributions are skewed to the right, which is caused by the occurrence of severe traffic congestion.

The BTI values for most off-peak periods (morning and evening) are less than 5% and occur in stable traffic conditions, whereas the BTI values increase sharply during peak-hour periods. In general, travelers require an additional 8–12% of the median travel time to travel on the route during peak

hours on weekdays, an additional 13–18% on Fridays, and an additional 10–25% on Saturdays and Sundays. Compared with weekdays and Fridays, weekends have significantly more extreme traffic conditions, with longer lengths and higher BTI values for travel time reliability. Compared with the average or median travel time, travel time variability is often low during off-peak hours and high during traffic congestion periods. Moreover, low travel time variability implies high travel time reliability and vice versa. Therefore, the findings for travel time variability and reliability coincide.

For the other two reliability indicators, the width indicator signifies similar patterns of the unreliability periods as BTI, whereas the skewness indicator shows more fluctuations because it measures the relative probability of extreme travel times, which is different from BTI.

We also show the estimated quantile functions of travel time and the reliability indicators BTI as departure time-of-day functions in Fig. 10(a) for the Yilan-to-Taipei route. The results for the Sonoma-US-101 route are illustrated in Fig. 10(b). The proposed methods provide analytical tools to obtain useful travel time information from historical data.

V. Discussion and Concluding Remarks

Assessing travel time variability and reliability is a long-standing topic in transportation research. The paper proposes a new methodology for quantifying travel time variability and reliability for a freeway using the aggregated travel time information in TDCS by linking fragmented travel time records of consecutive ETC gates. The major contributions of the proposed method for studying travel time variability and reliability are summarized as follows.

- The data-adaptive kernel density estimates at each time-of-day period efficiently summarize the travel time data with flexible shapes that are not restricted to a particular parametric density family and accurately reflect the spread and variability of travel time.
- The proposed FDA approach uses FPC analysis to summarize information of the conditional density functions at each time-of-day period using a few vectors of FPC scores. It effectively serves as a dimension reduction method from infinite-dimensional random functions to finite-dimensional vectors.
- The novel functional travel time density model (FTTDM), incorporating time-of-day effects as a covariate into the FPC analysis on the conditional density functions, successfully formulates the time-varying feature of the dynamic travel time variability and reliability.
- The quantile functions derived from FTTDM and the BTI functions of departure time are useful for depicting the time-varying variability and reliability of travel time, which are helpful for road users to identify peak traveling hours and to plan their trips.
- The conditional travel time density functions derived from FTTDM serve as a basis for performance evaluation that accounts for not only the length of travel time but also its variability and reliability, such as by defining the levels of service and evaluating the dynamic conditions of a transportation system.

In this study, BTI was used as the performance measure for travel time reliability, which is associated with the variability and quantiles of travel time. As the basis for deriving travel time distributions, the proposed FTTDM can also be applied to other reliability measures of travel time, such as statistical range methods, tardy-trip measures, and other probability measures [6].

In the case study, the route travel times vary with the departure time of day, and the peak hours of departure time differ across the four types of day. The spreads of travel time, as indicated in the estimated conditional probability density functions, increase significantly with travel time.

Numerous long travel times of the routes appear in the datasets. It may be of interest to investigate the causes of such outliers in travel times by linking the official records of traffic accidents to incidents on the freeways in future studies.

Finally, path travel time can be estimated in a path-tracking or a link-based manner. In this study, we obtain travel times by the weighted sum of link travel times and focus on the methodology of modeling variability and reliability of travel times. Comparisons with the path-tracking travel times could be of interest in future research.

Acknowledgment

The authors thank the editor, the associate editor, and anonymous referees for the constructive comments.

References

[1] S. H. Hamdar, A. Talebpour, and J. Dong, "Travel time reliability versus safety: A stochastic hazard-based modeling approach," *IEEE Trans. Intell. Transp. Syst.*, vol. 16, no. 1, pp. 264–273, Feb. 2015.

[2] J. Kim and H. S. Mahmassani, "Compound Gamma representation for modeling travel time variability in a traffic network," *Transp. Res. B, Methodol.*, vol. 80, pp. 40–63, Oct. 2015.

[3] S. Clark and D. Watling, "Modelling network travel time reliability under stochastic demand," *Transp. Res. B, Methodol.*, vol. 39, no. 2, pp. 119–140, Feb. 2005.

[4] L. M. Kieu, A. Bhaskar, and E. Chung, "Public transport travel-time variability definitions and monitoring," *J. Transp. Eng.*, vol. 141, no. 1, Jan. 2015, Art. no. 04014068.

[5] N. Uno, F. Kurauchi, H. Tamura, and Y. Iida, "Using bus probe data for analysis of travel time variability," *J. Intell. Transp. Syst.*, vol. 13, no. 1, pp. 2–15, Feb. 2009.

[6] J. W. C. van Lint, H. J. van Zuylen, and H. Tu, "Travel time unreliability on freeways: Why measures based on variance tell only half the story," *Transp. Res. A, Policy Pract.*, vol. 42, pp. 258–277, Jan. 2008.

[7] C. Kamga and M. A. Yazıcı, "Temporal and weather related variation patterns of urban travel time: Considerations and caveats for value of travel time, value of variability, and mode choice studies," *Transp. Res. C, Emerg. Technol.*, vol. 45, pp. 4–16, Aug. 2014.

[8] W. Kou, X. Chen, L. Yu, Y. Qi, and Y. Wang, "Urban commuters' valuation of travel time reliability based on stated preference survey: A case study of Beijing," *Transp. Res. A, Policy Pract.*, vol. 95, pp. 372–380, Jan. 2017.

[9] F. Lei, Y. Wang, G. Lu, and J. Sun, "A travel time reliability model of urban expressways with varying levels of service," *Transp. Res. C, Emerg. Technol.*, vol. 48, pp. 453–467, Nov. 2014.

[10] H. Al-Deek and E. B. Emam, "New methodology for estimating reliability in transportation networks with degraded link capacities," *J. Intell. Transp. Syst.*, vol. 10, no. 3, pp. 117–129, 2006.

[11] R. B. Noland and J. W. Polak, "Travel time variability: A review of theoretical and empirical issues," *Transp. Rev.*, vol. 22, no. 1, pp. 39–54, Jan. 2002.

[12] Z. Zheng, S. Ahn, D. Chen, and J. Laval, "Freeway traffic oscillations: Microscopic analysis of formations and propagations using wavelet transform," *Transp. Res. B, Methodol.*, vol. 45, no. 9, pp. 1378–1388, Nov. 2011.
[13] H. S. Mahmassani, T. Hou, and M. Saberi, "Connecting networkwide travel time reliability and the network fundamental diagram of traffic flow," *Transp. Res. Rec.*, vol. 2391, pp. 80–91, Jan. 2013.
[14] F. Ferraty and P. Vieu, *Nonparametric Functional Data Analysis: Theory and Practice*. New York, NY, USA: Springer, 2006.
[15] J. O. Ramsay and B. W. Silverman, *Functional Data Analysis* (Springer Series in Statistics), 2nd ed. New York, NY, USA: Springer, 2005.
[16] H. G. Müller, "Functional modelling and classification of longitudinal data," *Scand. J. Stat.*, vol. 32, no. 2, pp. 223–240, May 2005.
[17] J. L. Wang, J. M. Chiou, and H. G. Müller, "Functional data analysis," *Annu. Rev. Statist. Appl.*, vol. 3, no. 2, pp. 257–295, Jun. 2016.
[18] J. M. Chiou, "Dynamical functional prediction and classification, with application to traffic flow prediction," *Ann. Appl. Stat.*, vol. 6, no. 4, pp. 1588–1614, Dec. 2012.
[19] J. M. Chiou, H. G. Müller, and J. L. Wang, "Functional quasi-likelihood regression models with smooth random effects," *J. Roy. Stat. Soc. B, Stat. Methodol.*, vol. 65, pp. 405–423, May 2003.
[20] J.-M. Chiou and H.-G. Müller, "Modeling hazard rates as functional data for the analysis of cohort lifetables and mortality forecasting," *J. Amer. Stat. Assoc.*, vol. 104, no. 486, pp. 572–585, Jun. 2009.
[21] H. Rakha and W. Zhang, "Estimating traffic stream space mean speed and reliability from dual-and single-loop detectors," *Transp. Res. Rec.*, vol. 1925, pp. 38–57, Jan. 2005.
[22] J. van Lint and N. van der Zijpp, "Improving a travel-time estimation algorithm by using dual loop detectors," *Transp. Res. Rec., J. Transp. Res. Board*, vol. 1855, no. 1, pp. 41–48, 2003.
[23] H. Kim, Y. Kim, and K. Jang, "Systematic relation of estimated travel speed and actual travel speed," *IEEE Trans. Intell. Trans. Syst.*, vol. 18, no. 10, pp. 2780–2789, Oct. 2017.
[24] Taiwan Area National Freeway Bureau. (Jan. 2019). *ETC Operation Status and System Performance*. [Online]. Available: https://www.freeway.gov.tw/english/Publish.aspx?cnid=1164
[25] (Jul. 2019). *Caltrans Performance Measurement System (PeMS)*. [Online]. Available: http://pems.dot.ca.gov/
[26] T. Hsing and R. Eubank, *Theoretical Foundations of Functional Data Analysis, With an Introduction to Linear Operators*. Hoboken, NJ, USA: Wiley, 2015.
[27] B. W. Silverman, *Density Estimation for Statistics and Data Analysis*. London, U.K.: Chapman & Hall, 1986.
[28] T. Lomax, D. Schrank, S. Turner, and R. Margiotta, "Selecting travel reliability measures," Texas Transp. Inst., College Station, TX, USA, May 2003. [Online]. Available: http://tti.tamu.edu/documents/474360-1.pdf
[29] E. Mazloumi, G. Currie, and G. Rose, "Using GPS data to gain insight into public transport travel time variability," *J. Transp. Eng.*, vol. 136, no. 7, pp. 623–631, Jul. 2010.
[30] J. Dong and H. S. Mahmassani, "Stochastic modeling of traffic flow breakdown phenomenon: Application to predicting travel time reliability," *IEEE Trans. Intell. Trans. Syst.*, vol. 13, no. 4, pp. 1803–1809, Dec. 2012.
[31] K. Yin, W. Wang, B. X. Wang, and T. M. Adams, "Link travel time inference using entry/exit information of trips on a network," *Transp. Res. B, Methodol.*, vol. 80, pp. 303–321, Oct. 2015.
[32] M. Fosgerau and D. Fukuda, "Valuing travel time variability: Characteristics of the travel time distribution on an urban road," *Transp. Res. C, Emerg. Technol.*, vol. 24, pp. 83–101, Oct. 2012.
[33] M. Rahmani, E. Jenelius, and H. N. Koutsopoulos, "Non-parametric estimation of route travel time distributions from low-frequency floating car data," *Transp. Res. C, Emerg. Technol.*, vol. 58, pp. 343–362, Sep. 2015.
[34] S. Yang, A. Malik, and Y. J. Wu, "Travel time reliability using the Hasofer–Lind–Rackwitz–Fiessler algorithm and kernel density estimation," *J. Transp. Eng.*, vol. 137, no. 8, pp. 509–519, Aug. 2011.
[35] J. Fan and I. Gijble, *Local Polynomial Modelling and Its Applications*. London, U.K.: Chapman & Hall, 1996.
[36] W. J. Conover, *Practical Nonparametric Statistics*, 3rd ed. New York, NY, USA: Wiley, 1999, pp. 428–433.

Jeng-Min Chiou received the Ph.D. degree in statistics from the University of California at Davis, Davis, CA, USA, in 1997. He is currently a Distinguished Research Fellow with the Institute of Statistical Science, Academia Sinica. He is also a fellow of the American Statistical Association and Institute of Mathematical Statistics. His research interests include statistical modeling and analysis, traffic flow theory, and data analytics in transportation systems.

Han-Tsung Liou received the M.M. and Ph.D. degrees in transportation and communication management science from National Cheng Kung University, Tainan, Taiwan, in 2008 and 2015, respectively. He is currently a Post-Doctoral Fellow with the Institute of Statistical Science, Academia Sinica. His research interests include intelligent transportation systems, travel demand analysis, and network optimization.

Wan-Hui Chen received the Ph.D. degree in civil and environmental engineering from the University of California at Davis, Davis, CA, USA, in 1998. She is currently a Professor with the Department of Transportation Management, Tamkang University. Her research interests include transportation safety, transportation planning, applied statistics in transportation, and intelligent transport and technology.